An integrated temperature control system for a 3D printed droplet generation microfluidic device HC-BAR Chip

By

Sheshank Bhatt

Bachelor of Technology, Punjab Technical University, 2014

A Report Submitted in Partial Fulfillment of the

Requirements for the Degree of

MASTER OF ENGINEERING

In the Department of Mechanical Engineering

University of Victoria, Victoria, BC,

Canada

An integrated temperature control system for a 3D printed droplet generation microfluidic device HC-BAR Chip

By

Sheshank Bhatt

Bachelor of Technology, Punjab Technical University, 2014

Supervisory Committee:

Faculty Supervisor: Dr. Mohsen Akbari

Committee Member: Dr. Andrew Rowe

ABSTRACT

A microfluidic chip is a small device which deals with a very small amount of fluid. It has microscale channels. It has been used in different fields of science like engineering, physics, biochemistry, etc. A droplet generator is a microfluidic device which is capable of generating small droplets which is used in different applications like drug delivery, cell trapping and gene analysis. Temperature control is an essential part of droplet generation, and it affects the generation of droplets. This project proposes a microfluidic chip design (HC BAR Chip) with a uniform distribution of temperature with no embedded heating equipment. The chip is capable of creating heating and cooling zones unaffected by each other with a flow-focussing droplet generation method. CAD software like Solidworks is used to design and COMSOL Multiphysics® software for the analysis.

Table of Contents

LIST OF FIGURES

LIST OF TABLES

ACKNOWLEDGEMENT

I would first like to express my profound gratitude to my supervisor Dr Mohsen Akbari for providing me the opportunity to study at the University of Victoria and for his supervision and support throughout my Master's program. His expertise and guidance have been instrumental in shaping this research and I am grateful to him for his kind advice on my research topic.

My sincere thanks also go to Dr Mahmood Razzaghi, a post-doctoral researcher at the University of Victoria for his generous assistance in identifying the layout of my project and reviewing and providing invaluable insight into my work. He also guided me from time to time and taught me the usage of 3D printing. Without them, I would have never learned as many things as I did here. I appreciate such invaluable help and guidance they gave me.

I would like to thank all my other professors, co-workers, friends and siblings who provided support during my studies.

I also want to thank the University of Victoria for letting me work and study for my master's in Mechanical engineering and appreciate for providing the resources and a conducive environment for my program and this project.

Lastly and most importantly, I would like to thank my parents who gave their continued love, cheers, and support through this journey. Undeniably, without them, it is not easy to achieve this milestone.

I. INTRODUCTION

Microfluidics is the field of science in which a small amount of fluid on a microscale is precisely controlled and manipulated. Fields like engineering, physics, chemistry, biochemistry, nanotechnology and biotechnology joined together to develop the microfluidic system which processes low volume to achieve multiplexing, automation and high throughput screening[1].

The precise handling of the low volume is done by using microstructured devices which are typically on the order of tens and hundreds of micrometres [2]. The major advantages of these devices include small footprints, low volume of sample and reagent requirements, short analysis times, and control over the process being performed. This facilitated miniaturization of the single or multiple lab-based processes and gave rise to the concept of 'Lab on Chip' which revolutionized the way of performing research and enhanced the quality of information obtained[3]. Microfluidic devices can also be found with different names such as microreactors, organ on chip and lab on chip in different published literature which suggest the application of the chip[4][5][6].

1.1 Fabrication of microfluidic chip

The fabrication method and the material of these devices depend on the application and the complexity of the design. These devices can be fabricated with a wide range of materials and there are many methods to fabricate them [7]. A typical method is forming channels on the surface of a solid substrate and then bonding it to another plate to seal the channels. Historically, silicon and glass were used via photolithography and wet etching methods[8]. Nowadays, polymer and elastomer chips are quite common due to their ease of use and rapid prototyping with the advent of 3D printing technology which is an effective method for

complex designs of microchannels [9]. Paper microfluidic devices are also developed and are in frequent use[10].

1.2 Various applications of Microfluidic chips

There are various applications of these devices apart from microreactors, organs and lab on chip can be in organic synthesis[11], radiopharmaceutical synthesis[12], environment[13] and food analysis[14], in forensic science[15], clinical diagnostic with immunoassays[16] and DNA analysis[17], point of care diagnostics[18], study of cell biology by trapping them in form of droplets or while still flowing[19][20]. It is a more accurate imitation of the living body compared to other methods of testing like flask-based culture method[3]. Drug delivery and discovery are widely exploring the usage of microfluidic chips [21].

1.3 Types of Microfluidic chip

Various types of microfluidic chips are being designed and used some of them are microfluidic hydrogel chip [22], 3D culture integrated microfluidic chip [23], microfluidic chip for the single cell analysis [24], microfluidic chip with detection instruments [25], microfluidic model organism [26], organ on a chip[5], and droplet microfluidic chip[20]. Figure 1 is a schematic diagram of the different types of microfluidic chips [39].

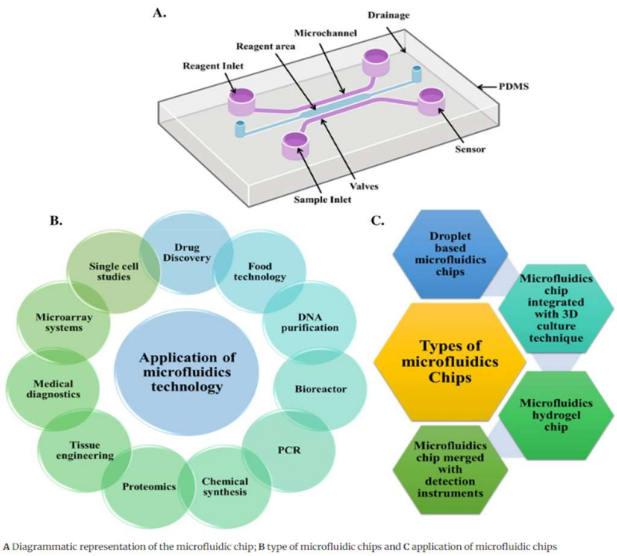

Figure 1: Types of the Microfluidic chip as per the design and application.
Reproduced with permission from Springer Nature

II. PROJECT OBJECTIVES AND OUTLINE

This thesis aims to design and develop a droplet-based microfluidic chip with both a Hot Zone and a Cold Zone which are unaffected by each other and have a uniform distribution of temperature along the target volume of the volume of interest without any localised heating effect or embedded system of heating.

The chip required below features:

1. The microfluidic chip must have provision to generate droplets.
2. A uniform temperature distribution is required both in the Heating Zone and Cooling Zone for the target volume.
3. The heating is required for the dispersed phase only in the Heating Zone and the cooling needs to be done after the droplet generation.
4. The design of the chip needs to have a proper inlet and outlet for the heating and cooling agent.
5. The Heating zone should have minimal effect on the Cooling zone in terms of temperature for which a design with the fins is proposed.
6. The design should be 3D printable at the University of Victoria.

III. DROPLET-BASED MICROFLUIDIC CHIP (DBM)

The main use of a droplet-based microfluidics (DBM) system is to take advantage of the unique volume of fluids that are naturally immiscible [27]. This technique allows the formation of thousands of droplets per second which are uniformly arranged and can be used for increasing the rate of analysis [28][29]. This technique is also being used to trap the individual cell with high throughput[28][30]. This technique can be used to observe and analyse cosmetics[31], diagnostic tests[32], air-filled fat particles [33] and controlled drug delivery[34]. A Schematic diagram for the typical droplet generator design is shown in Figure 2 [35]. A droplet generator requires two phases to create the droplets. These two phases are the continuous phase and the dispersed phase. The continuous phase is generally an oil and the dispersed phase is typically water.

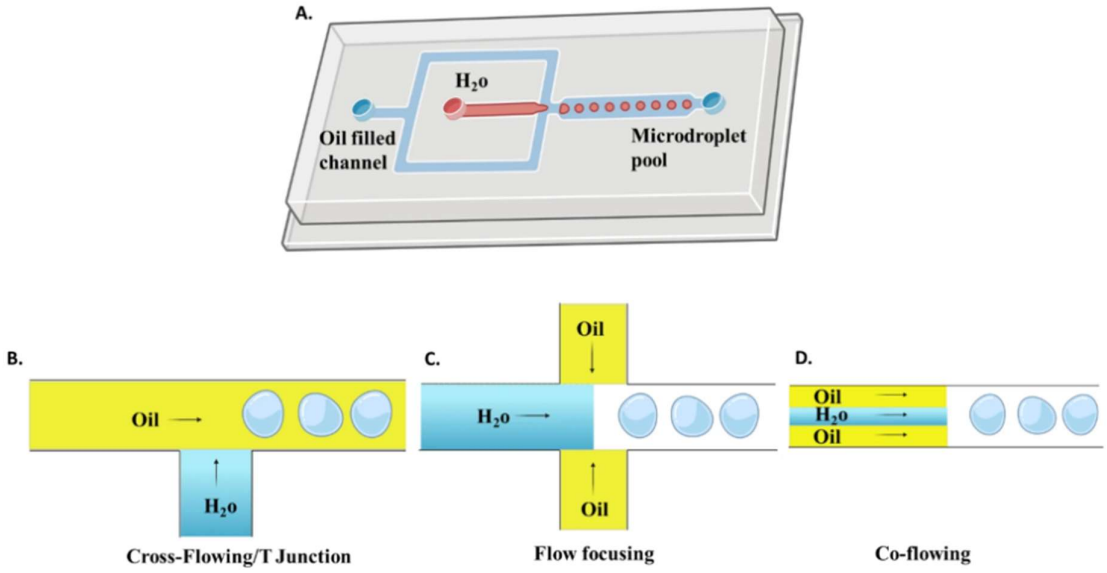

Schematic representation of a droplet-based microfluidics system. **A** Basic design and passive methods of droplet formation, **B** cross-flowing, **C** flow focusing, **D** co-flowing

Figure 2: A typical microfluidic droplet generator with different flow techniques.
Reproduced with permission from Springer Nature

In the treatment of colorectal cancer for the therapy, a drug delivery platform which was ph. sensitive is used[36].

3.1 Formation of the Droplets

In every chemical or biological experiment, precise control over the droplet formation process is a critical component. Controlling droplet volume, generation frequency, interface stability, and solute retention are particularly important. The droplet formation technique incorporates two necessary phases of fluid which are the continuous and dispersed phases. The droplet can be generated by the active or passive flow method.

The active flow method involves some external energy such as electric, magnetic or centrifugal energy[27][28][30]. Although active methods offer a higher level of control over the process, they usually require complex control equipment and create droplets at low generation frequencies[37]. The passive flow on the other hand does not depend on external energy. Typical designs of passive flow include cross-flowing designs (T junction), flow focusing and co-flowing methods which simplify the device. Figure 2 depicts the fundamental differences in them [38][39][40].

- Crossflowing (T-Junction): In this approach, the dispersed (water) phase is connected to the continuous flow at 90 degrees which forms a T junction.
- Flow focusing: In this approach, the dispersed phase (water) flows in the middle channel and is enveloped by the two continuous (oil) streams coming from either side.
- Co-flowing: It consists of three-dimensional flow-focussing geometry. It is a small capillary inside another capillary. The inner capillary has water and the outer capillary has oil. The co-flowing approach uses lithography to be fabricated.

Microfluidic droplets are most commonly created utilising flow-focusing and T-junction geometries. They are simple and can be used to produce different droplet sizes with uniform size distribution. These geometries are easy to fabricate and have a high droplet generation rate. Cross-flowing techniques are not favourable when the droplet needs to be smaller than the downstream channel[41].

IV. TEMPERATURE CONTROL IN MICROFLUIDIC SYSTEM.

The microfluidic chip requires multiple integrated functions in a small compact chip which is portable and can deliver rapid data output. The regulation of temperature in microfluidic systems plays a critical role in managing physical, chemical and biological applications and reactions. The temperature control in microfluidic chips has many advantages like a small amount of energy requirement, a simple system to control the temperature and short control time which is due to small volumes and large surface-to-volume ratio[42]. The change in the temperature in some experiments is not suitable and can affect the results of the experiment. Hence, different heating and cooling systems are developed to achieve precise temperature and control it. The typical method of heating includes the Peltier method, Joule Heating, microwaves, endothermal chemical reactions and integrated wires and lasers. These methods are used together with several sensors embedded in the microfluidic chip for continuous monitoring one such example of a sensor system is the use of thermocouples and Thermistors[43].

4.1 Importance of Temperature control

Temperature control or regulation generally refers to maintaining the temperature between a range of temperatures (all the readings between minimum and maximum allowed value). It is of high importance to heat or cool the target volume when the temperature is unwantedly increasing or decreasing from the required value between the range or when the sample needs to heat up or cool down, also control over the temperature gradient is crucial for some reaction and for the performance of the microfluidic device [43]. Many reactions such as Polymerase chain reaction (PCR), gene analysis, temperature gradient focusing of electrophoresis (TGF), digital microfluidics, and protein crystallization are highly sensitive towards temperature change [42]. Other examples which need temperature control are Recombinase polymerase amplification (RPA), phenotypic bacterial classifications and antibiotic susceptibility tests,

denaturation of proteins, nucleic acids amplification, microreactor, biochemical synthesis, cell culture and imaging, bubble generation, particle trapping, sweat analysis and atmospheric ice nucleating particle analysis [43].

4.2 Effect of Temperature on Droplet Generation in DBM

Droplet size control is very crucial for microfluidic applications in biology, chemistry, and medicine. Many factors, including the composition of the fluids, the surfactants, the flow rate ratio, the viscosity ratio, microchannel shape, and other dimensionless quantities, influence the droplet's size. It has been observed that the droplet size decreases if the continuous to dispersed phase (oil to water) flow rate ratio increases and vice versa[44]. The formation of droplets in passive method microchannels relies on the shearing and extrusion mechanism of the fluid and is contingent upon the operational circumstances. Keeping continuous phase flow rate and viscosity constant, the droplet size increases with the increase of dispersed phase flow rate but the formation rate of the droplet decreases. The droplet size decreases and the formation period (spacing of droplets) increases with the increase of the viscosity of the dispersed phase[45]. So, when the dispersed phase is heated, the viscosity of the dispersed phases is reduced which results in an increased formation rate but the size of the droplet decreases. Hence, the droplet size and droplet generation rate can be controlled by regulating and maintaining a uniform temperature of the dispersed phase.

V. LITERATURE REVIEW: EXISTING DESIGN AND ANALYSIS

The temperature gradient is generated due to localised 2-dimensional heating methods and layer-by-layer fabrication of 3-dimensional microfluidic chip. This results in uneven heating of the target volume[46]. Advanced 3D printing methods have facilitated to production of complex designs which can support 3 3-dimensional heating around the target volume.

Derek et. al. suggested three different geometries to support the 3-dimensional heating of the target volume. The geometries were identified by maintaining the heating channel's orientation distinct and keeping the target volume at the centre of the heating channel. The target volume in one of the geometries was placed at the centre of three concentric heating channels and the centre of the helical heating channel in another one. Using COMSOL Multiphysics® software, it was determined that a helical channel is more efficient in maintaining uniformity of temperature along the target volume than concentric parallel channels[47].

Troy et. al. explores and analyse three new 3D heating geometries keeping the target volume at the centre of the heating channels and eliminating the weakness of the heater geometries created by the traditional means. These designs were more isothermal over a long spatial range. All the models were designed in 10 mm × 5 mm × 5 mm solid space and COMSOL Multiphysics® software was used for finite element analysis. Serpentine, helical and box heating channels were designed and in order to make uniform temperature distribution these designs were modified to 3D serpentine, tapered helical and diamond designs as shown in Figure 3.

The tapered helix has one of the smallest temperature differences along the volume of interest and it was also able to avoid any temperature bump and has one of the longest lengths of isothermal temperature. It was also considered as median in terms of the temperature difference along the isothermal length.

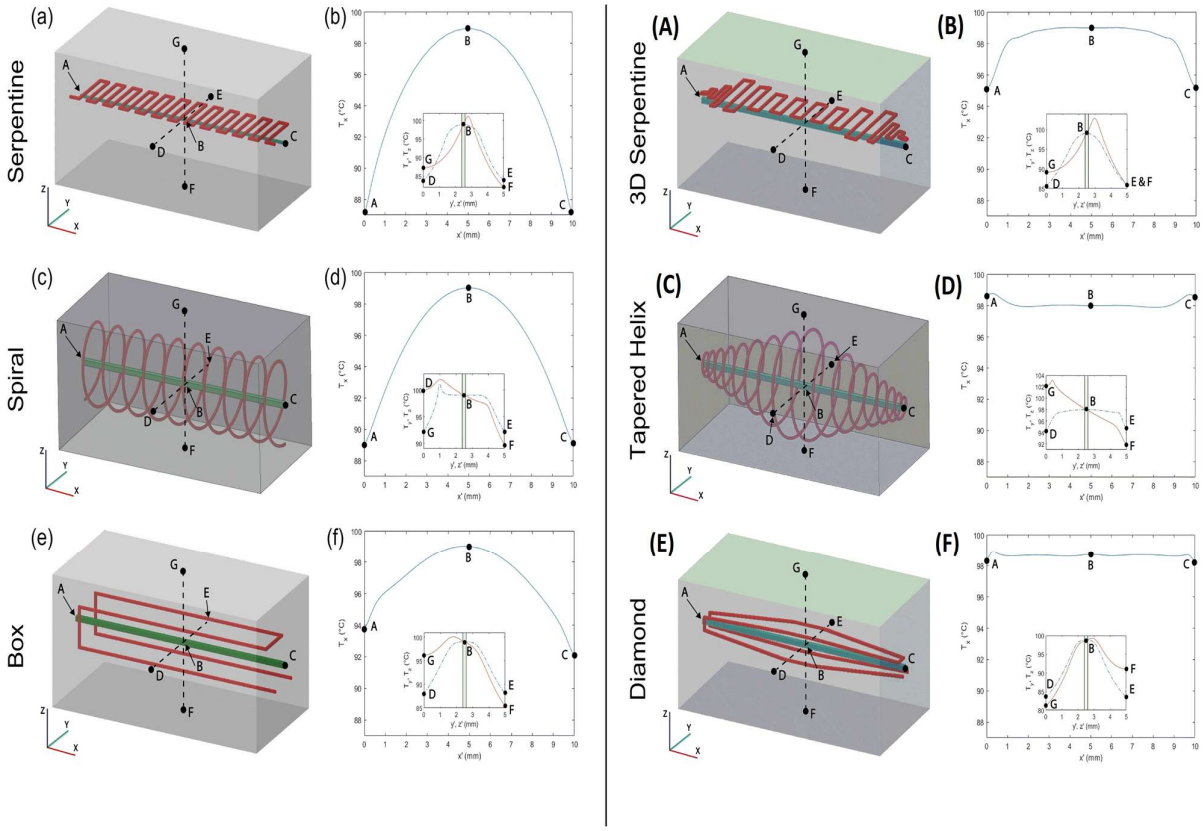

Figure 3: Different designs analyzed by Troy et. al.

"Used with permission of Royal Society of Chemistry, from 3D Printing-Enabled Uniform Temperature Distributions in Microfluidic Devices, Troy et. al., 22,2022; permission conveyed through Copyright Clearance Center, Inc."

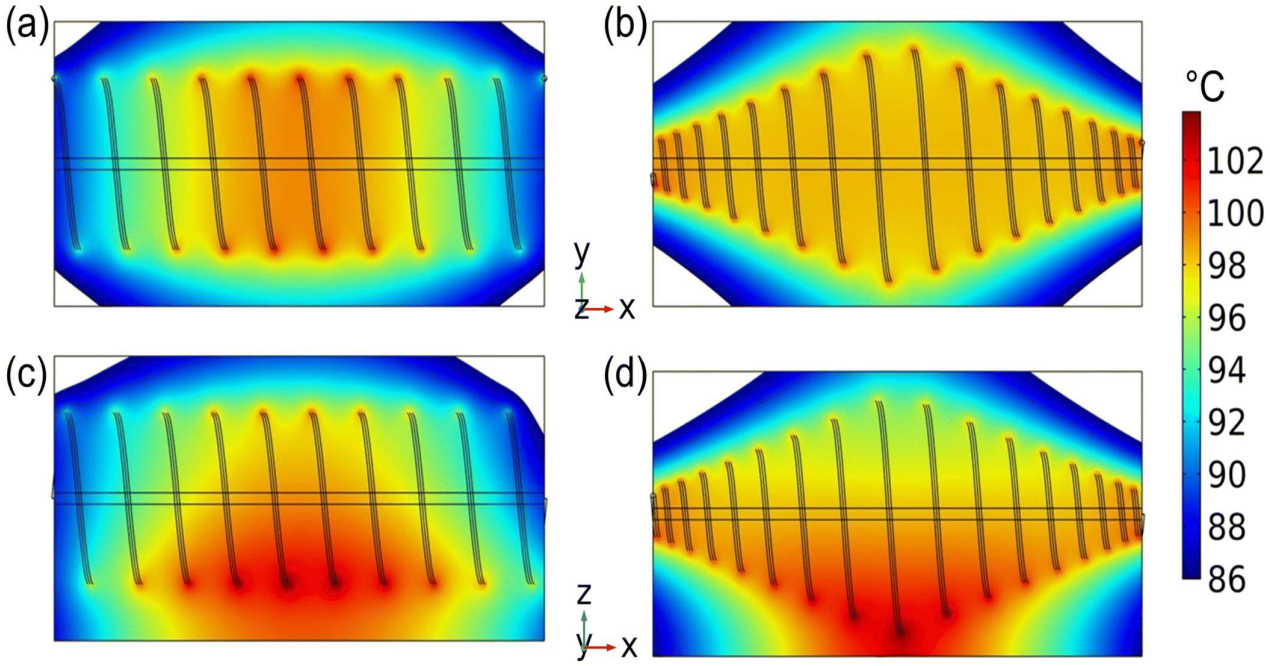

Figure 4: Temperature map plots of (a and c) the spiral and (b and d) the tapered helix.

"Used with permission of Royal Society of Chemistry, from 3D Printing-Enabled Uniform Temperature Distributions in Microfluidic Devices, Troy et. al., 22,2022; permission conveyed through Copyright Clearance Center, Inc."

The internal temperature distribution of helical and tapered helical design as top view in Figure 4 a & b respective and side view Figure 4 c & d respectively is shown. The helical heater chips exhibit a low degree of spatial temperature homogeneity as evidenced by the target volume that changes colour over time. There are fewer colour variations in the target volume of the tapered helix, indicating better spatial temperature uniformity [48].

VI. METHODOLOGY

To design a chip with both heating and cooling zones which can maintain the isothermal temperature at the target volume first literature review was done on different Droplet-based microfluidic chip designs and temperature control microfluidic chip designs to understand the droplet generators and traditional methods of heating and temperature control in microfluidic system.

The modeling of chip design was done in computer-aided design (CAD) software SOLIDWORKS keeping the specification and printing volume of 115mm x 65mm x 165mm (4.52″x2.56″x6.1″) into consideration of the 3D printer Anycubic Photon S.

The resulting design was converted to the step file and was analysed in COMSOL Multiphysics® software for finite element analysis. COMSOL and MATLAB® plotting features was used to plot the temperature distribution for the result.

The results can be validated by printing the chip and measuring the temperature distribution with the help of an infrared camera (IR camera).

6.1 Selection of Droplet generation method

It was conceived that the passive method of droplet generation neither makes the design complex nor requires many types of equipment. In the passive droplet generation method Flow focussing and T junction were easy to fabricate and had a high droplet generation rate. The droplet size can be controlled by maintaining the flow rate of the dispersed phase constant and maintaining the required viscosity by heating the dispersed phase channel (Section 3.1 and Section 4.2). Initially, HC-BAR Chip modelling was done by considering the T-junction droplet generator and initially by heating both the continuous and dispersed phases as shown in Figure 5. Flow-focussing droplet generator was selected as the desirable droplet generator method after further modelling and change in design to achieve the desired result after simulations.

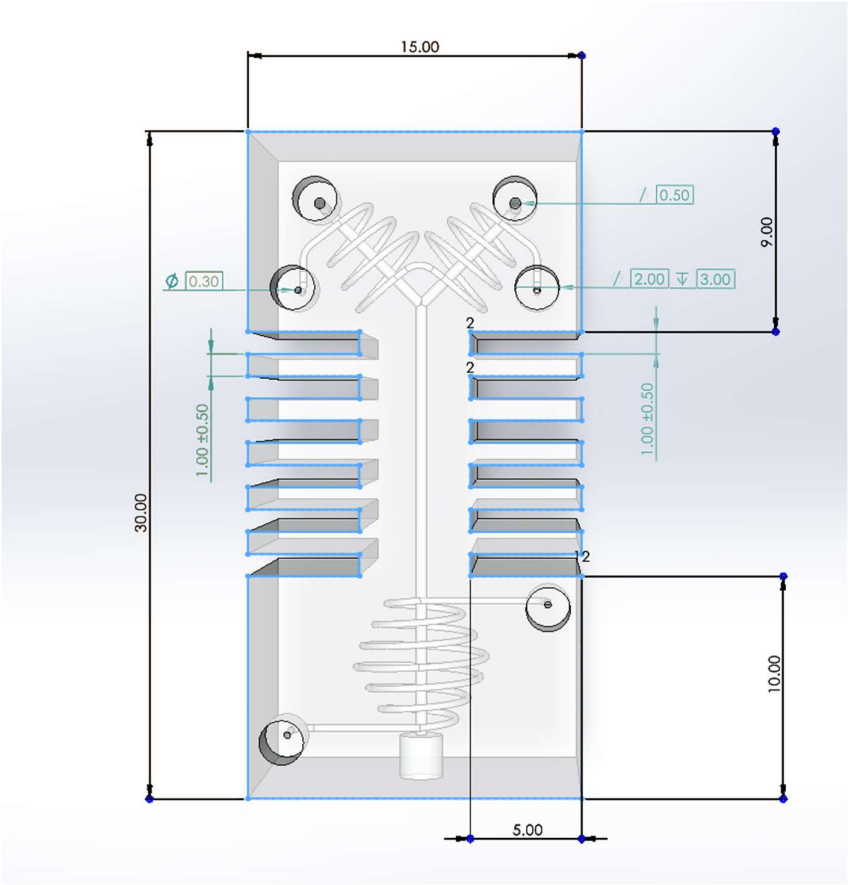

Figure 5: Top view of the initial design of HC-BAR Chip with dimensions with T-Junction droplet generation method and tapered helical heating and cooling channels.

6.2 Selection of Heating channel design

Regarding the design for the isothermal temperature, in addition to having the longest duration of isothermal temperature and the smallest temperature differential throughout the volume of interest, the tapered helix was also able to eliminate any temperature bumps. It was also regarded as the median for the temperature variation along the isothermal length (Section 5). Therefore, the tapered helical design of the heating and cooling channel was preferred for this project. Other designs can also be selected based on the application and desired results.

VII. DESIGN FOR HC-BAR CHIP

The HC-BAR Chip stands for Hot and Cold Bhatt-Akbari-Razzaghi Chip. The Chip has a heating and cooling zone separated by serpentine space for the target volume which acts as a fin and keeps the heating and cooling zones unaffected by each other as shown in Figure 6. In other words, to separate the heating zone from cooling zone.

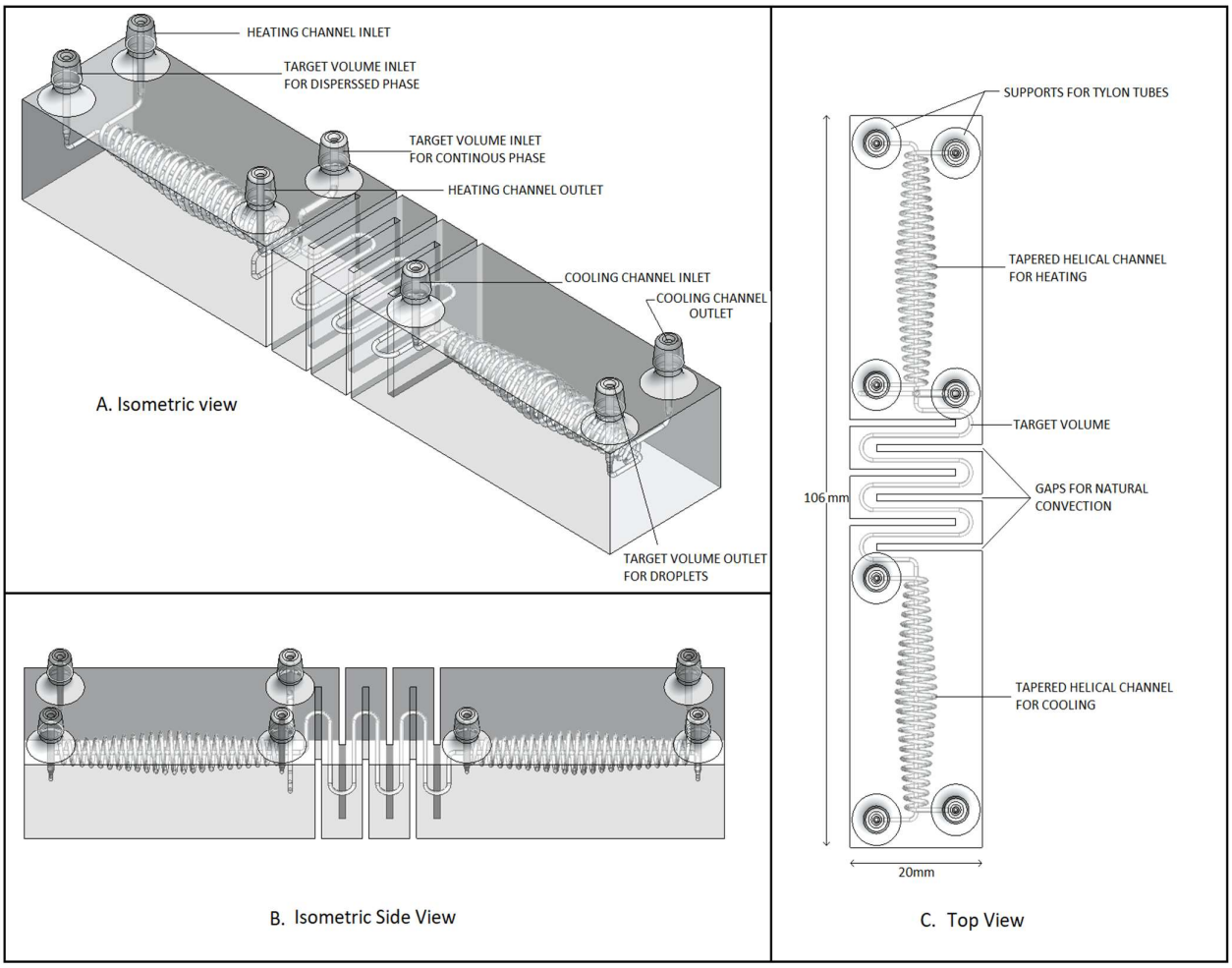

Figure 6: HC-BAR Chip A) Isometric View B) Isometric side view C) Top view.

The Fins in the Chip were made in serpentine manner to dissipate the heat and in order to increase the length of the conduction area design as shown in Figure 6. The other reason to adapt the serpentine design was to make the chip printable at University of Victoria and keeping printability of Anycubic Photon S printer available in the Lab. It also has a provision to produce droplet and inlet for the continuous phase.

All the channels were kept as of 600 µm in diameter which is easily 3D printable by Anycubic Photon S 3D printer and the Chip is 106mm in length and 20mm in height and width. The volume of interest or the target volume is kept running through the central axis of the chip. Heating and cooling channels were modelled in tapered helical design around the target volume for the uniform distribution of temperature. Connectors were added to the modelling in order to connect Tygon tubes for a functional model. The connectors add a height of 6.5 mm to the Chip and are tapered from 1.7mm to 2mm wide. At first the target volume was taken as 300 microns but due to printability constraint it was increased to 600micron. The heating and cooling channel were also kept as 600 microns as it is the least printable channel dimension by printer. A rough calculation was done on understand the smallest helical di and largest effective helical dia which came to be 3mm and 6mm from the target volume.

Table 1: Design Parameters of the HC BAR Chip

Parameters	Dimension
Microfluidic Chip dimension	(L x B x H) 106mm x 20mm x 15mm
Height of Tygon Tube connectors	6.5mm
Heating and Cooling Helical Channel Dia	600 microns
Target Volume Cross section	600-micron dia (circular)
Angle of Helical channel elevation till centre	5 degree
Smallest Dia of Helical Channel (At ends)	3mm
Largest Dia of the Helical Channel (Middle)	6mm
Pitch of the Helix	1.4mm
Number of helical revolutions per helix	24

The helical angle is kept at 5 degree according to length of helix and keeping 3mm as dia at the edge of the helix and 6mm at the centre of the helix. This angle was at 30 degree when the

chip length and helix length were small. All the features of the chip are tried to keep 1mm for the easy printability Hence the pitch of the helix was maintained at 1.4mm. The gap between the chip's serpentine path is 1mm and is considered to be filled with air therefore it is used as a boundary condition of natural convection during the analysis by keeping the flow rate of air at 0mm/s. The material of the chip was considered as PDMS from the database of the software as it closely represents the material properties and has the closest thermal conductivity of the resin used in the printer which is 0.16 W m^{-1} K^{-1}.

The heating and the cooling liquid were considered as water for the simulation and the target volume was also considered as water for the ease of simulation with a fluid flow rate of 2mm/s in every channel and the properties of the water were used from the built-in database of the software. No other properties were changed from the default settings. The temperature of the water in the heating and cooling channels was considered as 70°C (343.15 K) and 1°C (274.15 K) respectively. A mesh size was considered as of 'Fine' element as per the software was applied to the geometry.

The design and simulation parameters can be changed and actual values for the thermal conductivity of the resin can be used which can be calculated after practical analysis, the chip and values for convection heat transfer coefficient for the different liquid inside target volume, heating channels and cooling channels can be added to the simulation software as required by the user.

VIII. ANALYSIS WITH COMSOL

COMSOL Multiphysics® software was used to analyse the design and for the simulation. The Microfluidic module of the COMSOL Multiphysics® software facilitates easy operation and study of microfluidic systems. It can be simulated for the creeping, laminar, porous media, multiphase, and slip flow, and it can solve stationary and time-dependent flows in 2D and 3D. It also has the feature of combining another module which can be used to study the structure interaction and thermal flow [49].

8.1 Simulation Parameters and Boundary Conditions

For this design, time-independent and stationary as the study step was selected. COMSOL's study module 'Laminar flow' was selected as the flow in the channel is very slow and the diameter of the channel is in microns this results in a very low Reynold's number. For the study of heat distribution 'Heat transfer in solid and fluid' module is selected together with the 'Non-isothermal' Multiphysics study module to do the study for the temperature distribution along the target volume. For the Laminar Flow study inlet velocity is considered as 2mm/s and the gap is considered as open boundary. For the Heat Transfer study, the temperature for the target volume is considered 293.15 K (20°C), for the heating channel, is 343.15 K (70°C) and for the cooling channels it is kept as 273.15 K (1°C). The material of the HC-BAR Chip is considered to have PDMS with 0.16 W $m^{-1}K^{-1}$ thermal conductivity which resembles the property of the Anycubic Acrylic resin in terms of thermal properties and water is selected from the in-built database as the liquid for the target and heating and cooling channels.

8.2 Simulation results

It is observed that the design of the HC BAR Chip is capable of creating two different zones without affecting each other as shown in Figures 7 A & B. It can be observed that the serpentine path is light yellow at the start and becomes white before entering the cooling zone. It is also observed that the light blue colour appears before the target volume enters the cooling zone

from which we conclude that the cooling zone is unaffected by the temperature of the heating zone and the efficiency of both zones is not compromised due to each other.

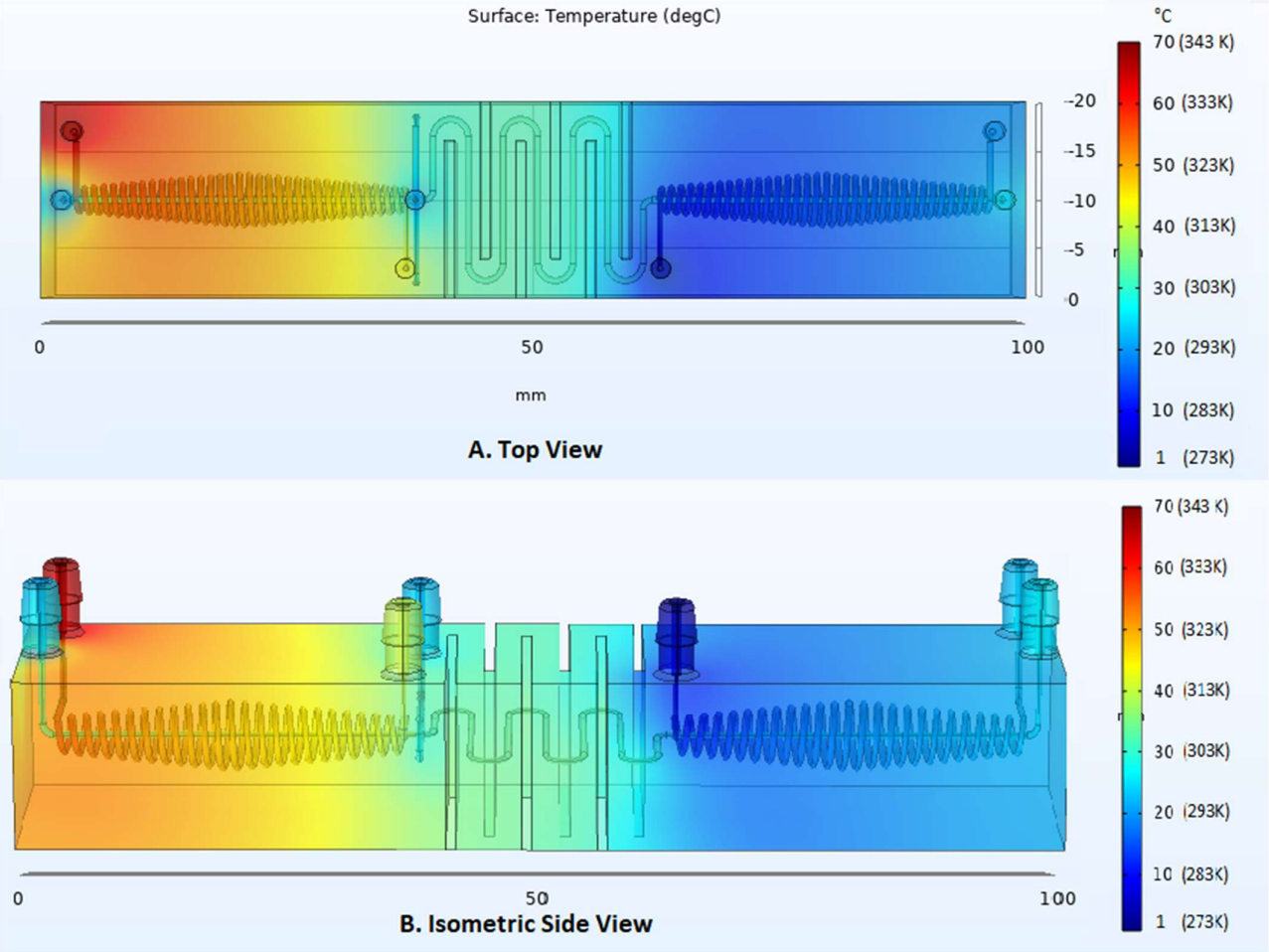

Figure 7: Simulation result for the HC-BAR Chip from A. Top view B. Isometric View

In order to get the thermal distribution target volume is extracted out of the design after simulation which is shown in Figure 8 'A' which depicts the temperature distribution along the target volume which is the result of the effect of Heating and cooling channels. A graph is plotted along the target volume centre line with the help of COMSOL and MATLAB® plotting features. The temperature distribution along the centre line along the target volume is almost uniform and is maintained within a difference of 1°C (2K) in both the heating and cooling Zone as shown in Figure 8 'B'.

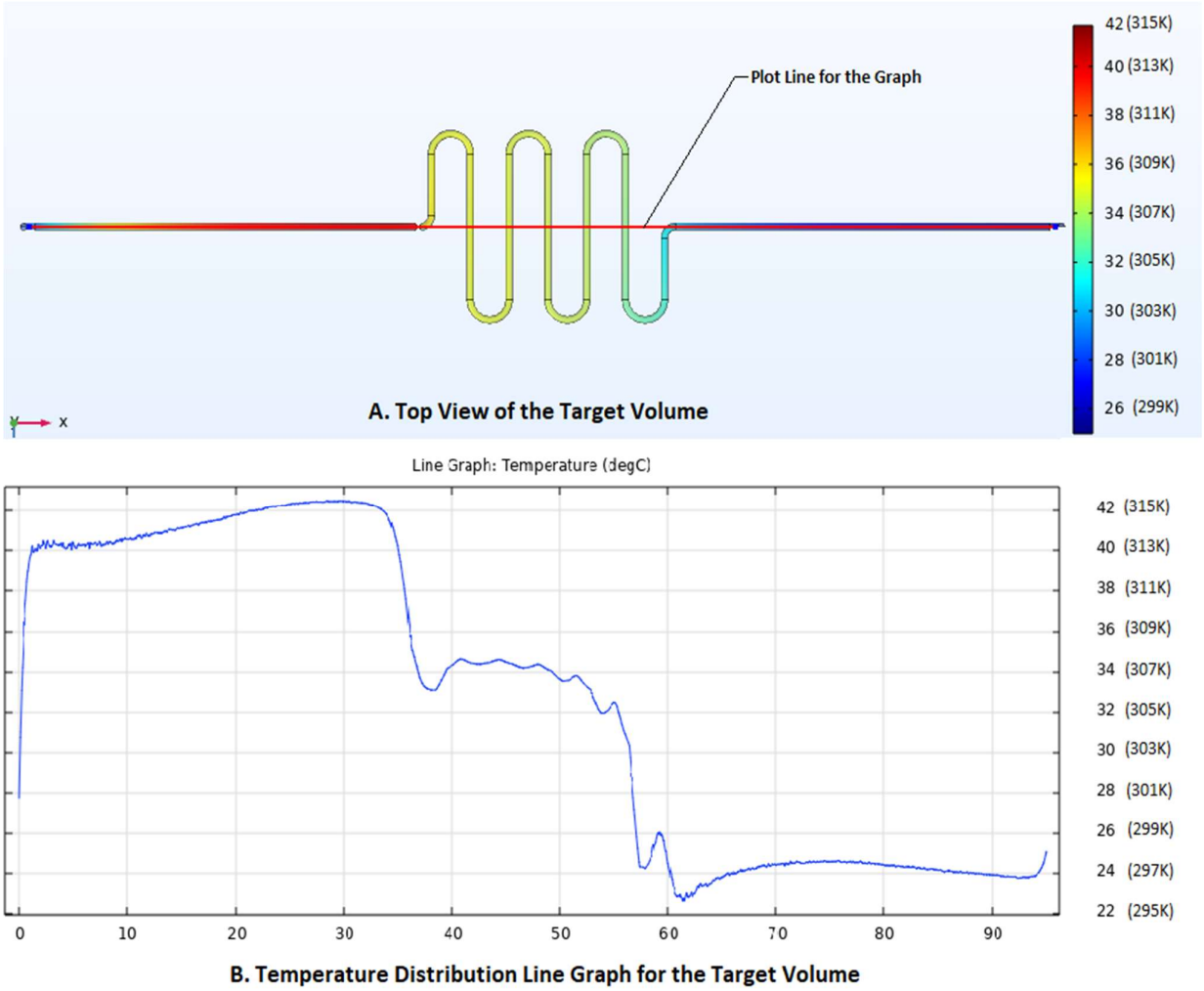

Figure 8: Simulation result for the Temperature distribution along the target volume A. Top view of the Target Volume B. Line Graph for Temperature Distribution through the centre line along the Target Volume.

As per the Graph shown in Figure 8 'B' it can be seen that as the fluid reaches the heating zone there is a sudden rise of the temperature due to the heating zone which is maintained till the heating zone until the continuous phase channel connects to the dispersed phase. There is a sudden drop in temperature due to the introduction continuous phase which reduces the temperature by 8 to 10 degrees or kelvin. This temperature is further reduced to 7 to 8 degrees or kelvin when the target volume enters the cooling zone and then the temperature is maintained until the target volume leaves the cooling zone. It is proposed that the temperature can be further reduced with the use of other coolant than water.

IX. Sensitivity analysis

Figure 5 show the initial design of the HC-BAR chip which after further research and sensitivity analysis is modified to its final design as shown in Figure 6.

The sensitivity analysis was done on below mention parameter to analyse the effect on temperature distribution:

9.1 Parallel vs Tapered helix

Simulation result for the temperature distribution in Chip with parallel and tapered helical heating and cooling channels in Figure 9 and as graph in Figure 10 are presented. As per the result it can be concluded that the uniformity of the temperature distribution is better in tapered helix as compare to the parallel helix.

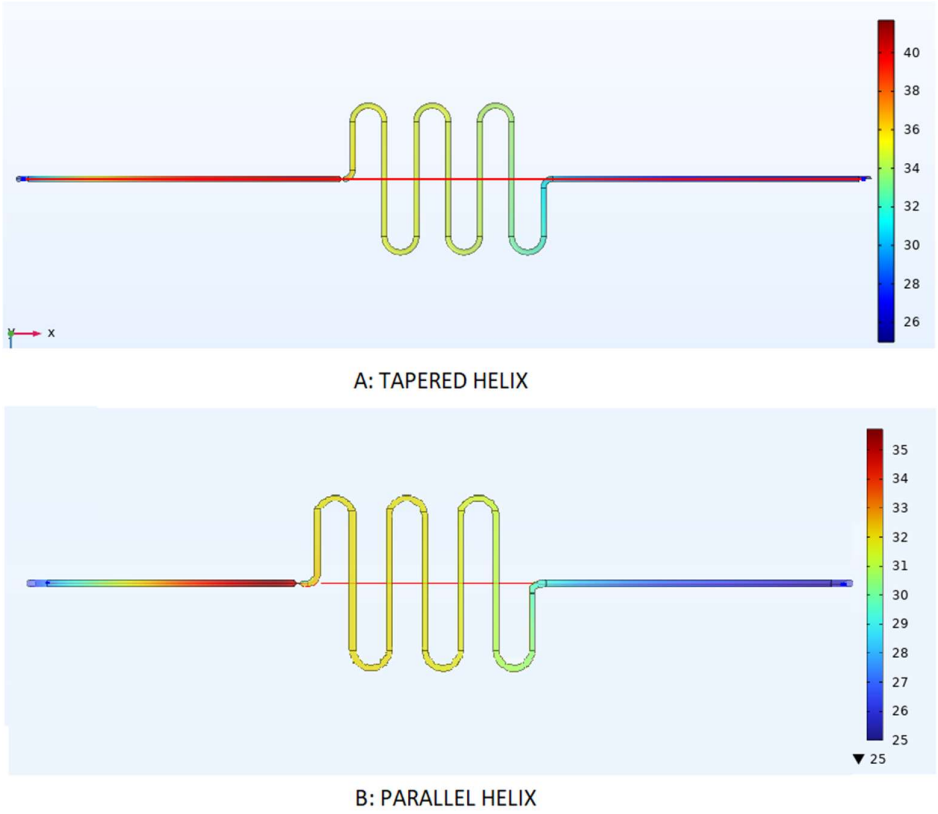

Figure 9: Temperature distribution in Tapered and Parallel helical channel HC-BAR Chip

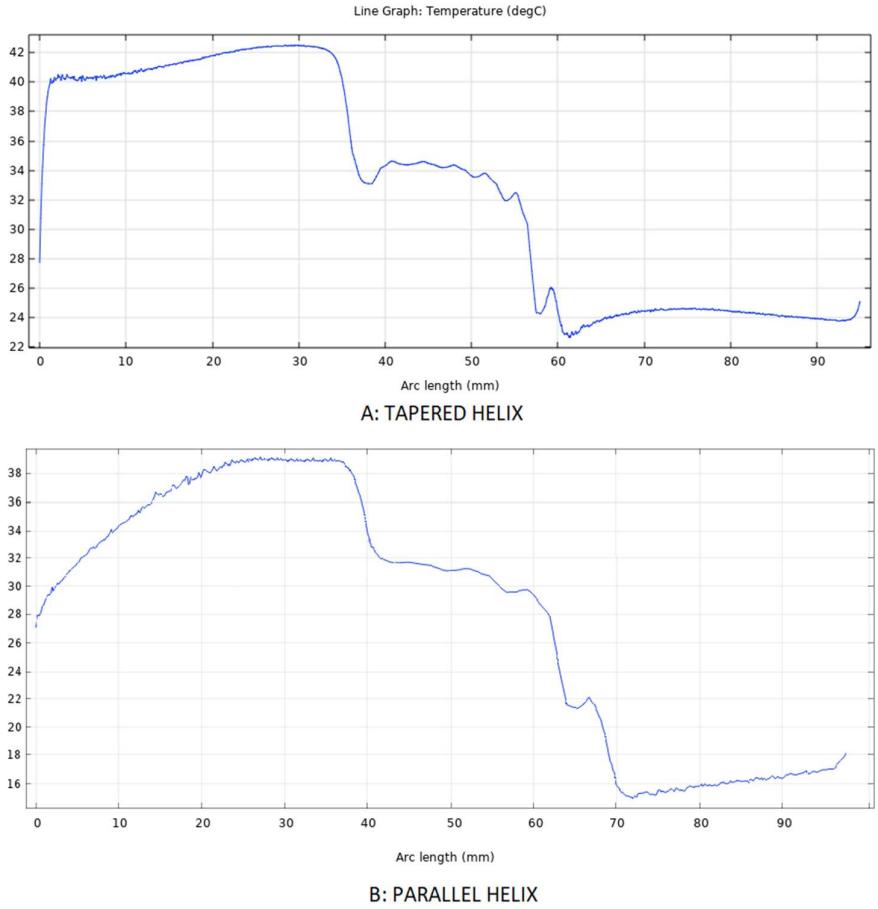

Figure 10: Graph showing the temperature distribution for the HC-BAR Chip with Tapered and parallel helical channels.

In parallel helical channel chip, the temperature gradient can be seen rises from 28 °C to 38 °C from the beginning of the channel to 25mm, after that there is some uniformity until continuous phase is added. In tapered helical channel chip, the uniformity of the temperature distribution is maintained from almost beginning to the point where continuous phase is added to the form droplets and it is same for the cooling channels as well.

9.2 Effect of Length helical channel

Result for the different length of the microfluidic channel has been shown in Figure 11 and in graphical representation in Figure 12. It can be observed that the 100mm Chip is able to raise the temperature higher than 60mm temperature.

It can be observed that the 100mm microfluidic chip is able to raise the temperature by approx. 20°C on the other hand 60mm microfluidic chip was able to the raise only 5.4°C which

comparatively very less. It can also be noted that this chip was designed considering the printability of 'Anycubic Photon S' which can print as long as 115mm chip.

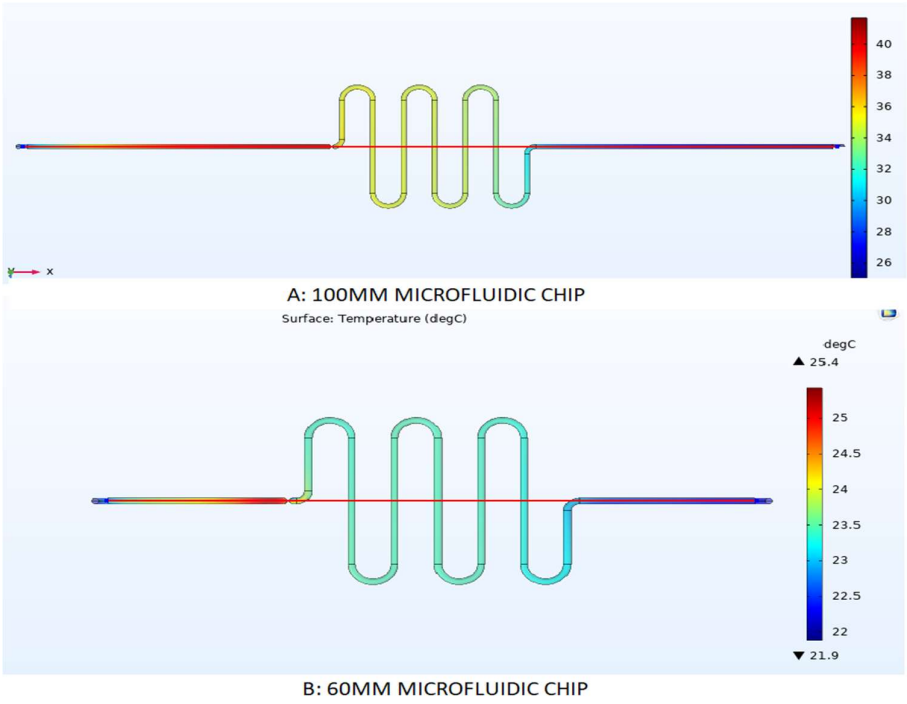

Figure 11: Simulation result for the 100mm long and 60mm long HC-BAR chip

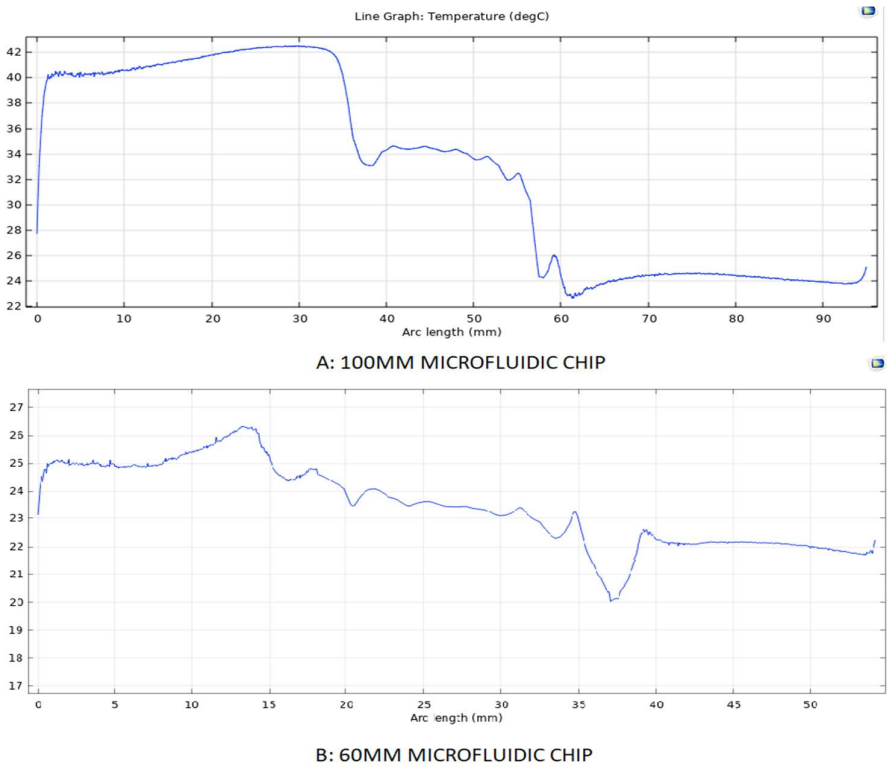

Figure 12 Graph for the simulation result for the 100mm long and 60mm long HC-BAR chip.

It can be noted that the max average temperature 25.25°C and min average temperature is 20°C for 60mm Chip and max average temperature 41°C and min average temperature is 23°C for 60mm Chip. Hence, we can say that efficiency of the 100mm chip is better in terms of raising and lowering the temperature.

9.3 Effect of Angle of the helix

It can be observed from the graph shown in Figure 13 which depicts uniformity of temperature and control of temperature by 5 degree and 10-degree tapered angle of HC-BAR chip.

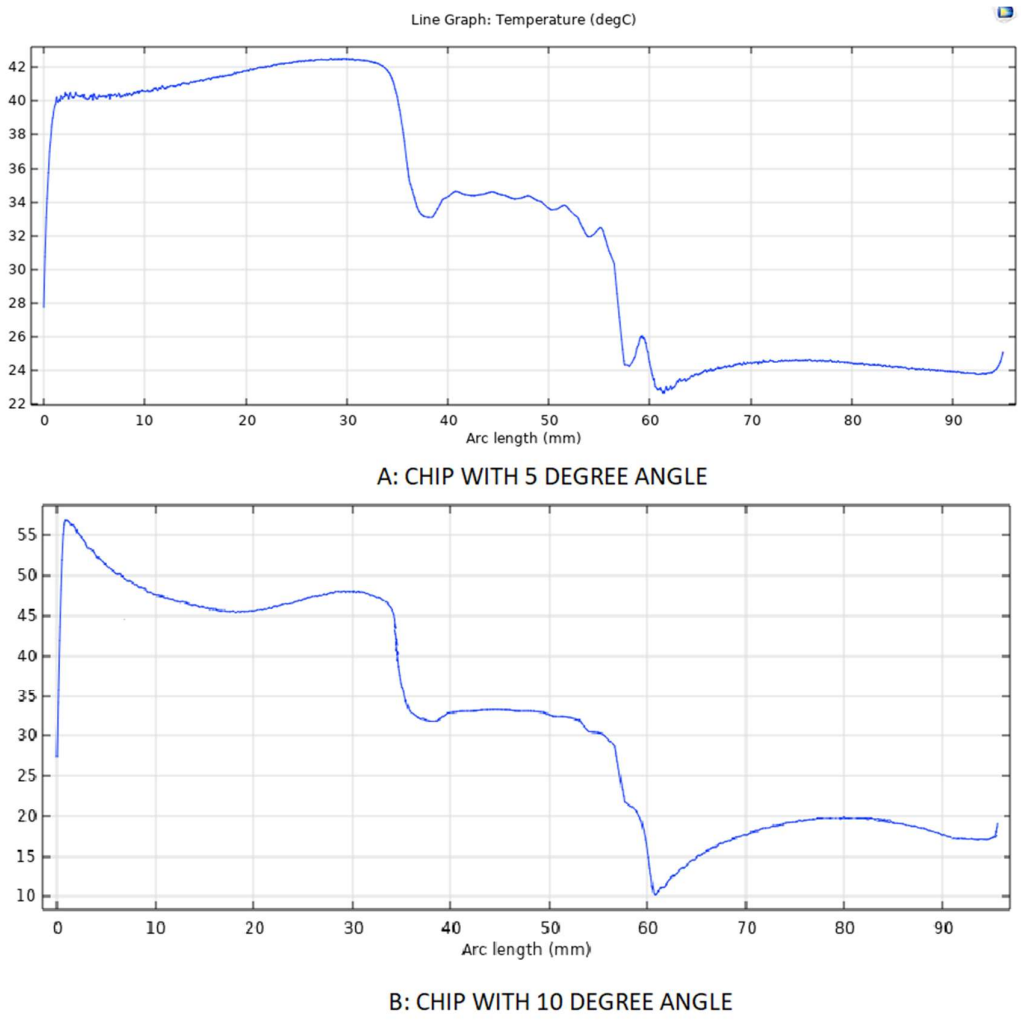

Figure 13: Graph plotted from the simulation result of 5-degree helical angle Chip and 10-degree angle helical HC-BAR chip

It can be noted that the uniformity of the temperature distribution was maintained by 5-degree angle and on the other hand the 10-degree tapered helical angle HC BAR has the same elevation of the temperature at start but is not efficient to maintain the isothermal temperature.

9.4 Design of the fin

Initial design of the HC-BAR chip is shown in the Figure 14 which has a standard fin. It can be seen that the distance for the target volume for the Heating zone to the cooling zone is very small which provide very less time to dissipate the heat from the fins.

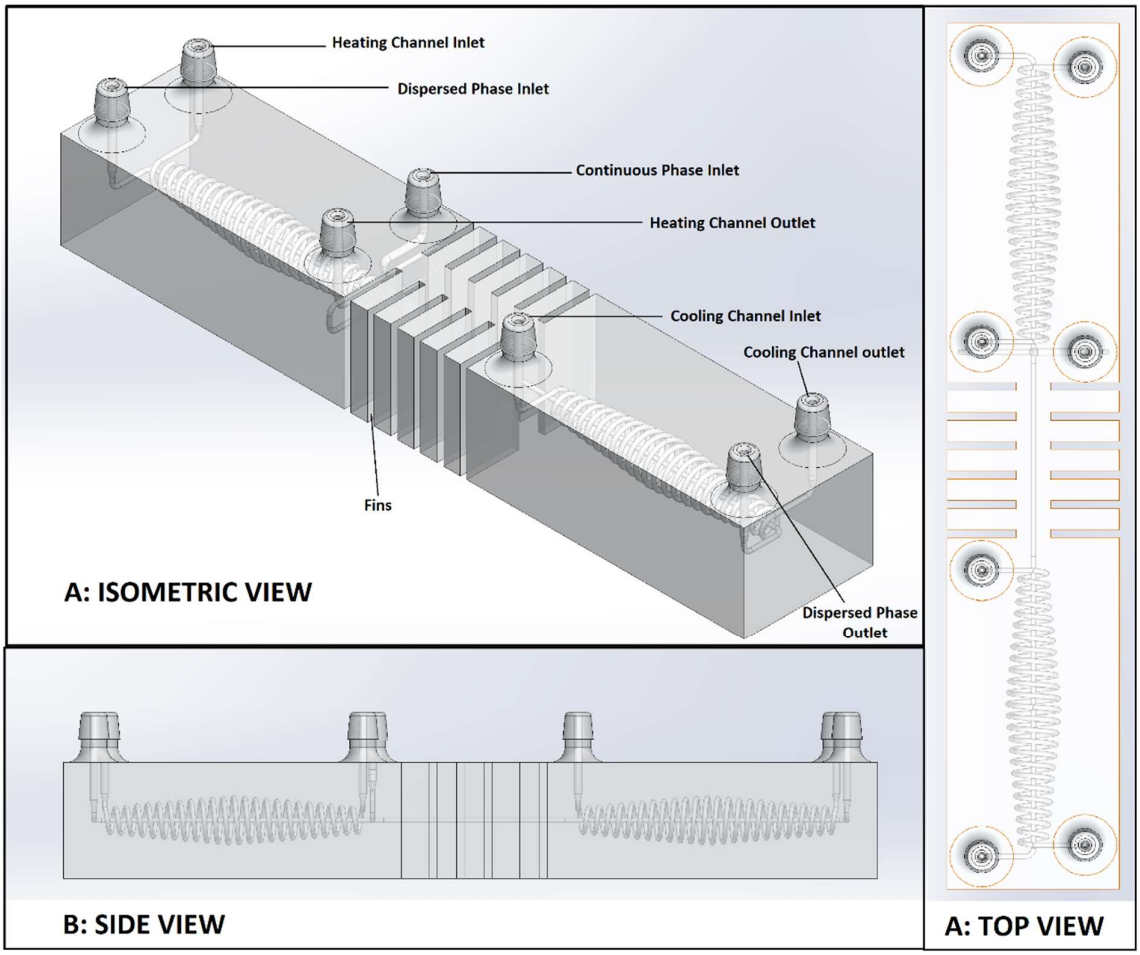

Figure 14: Different view of HC-BAR Chip with the Standard Fins

In the Figure 6 it can be observed that the introduction of the serpentine channel has provided longer length and more time in same amount of area and the fin work as insulation to reduce the impact of heating and cooling zone on each other resulting in increased efficiency.

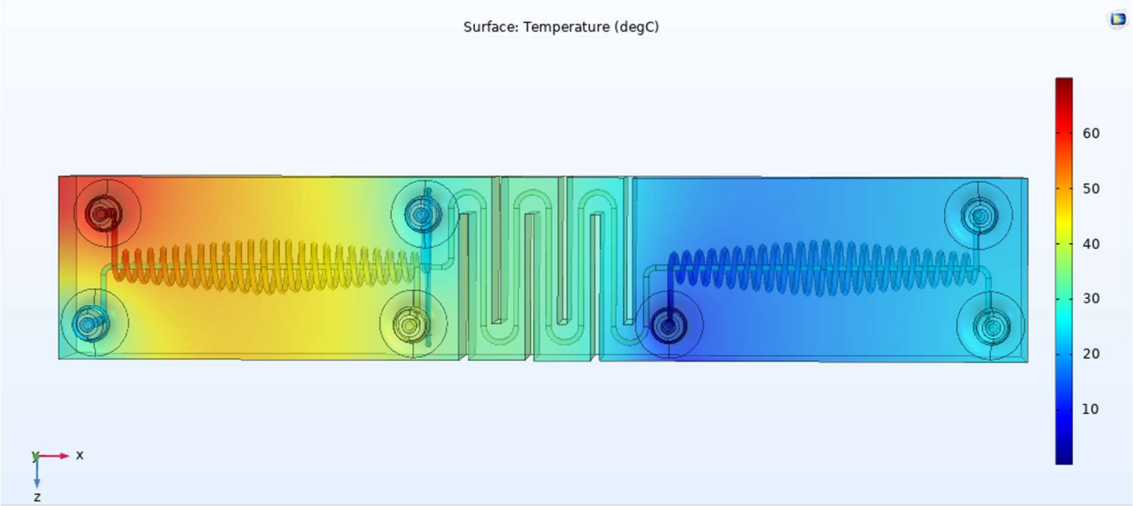

Figure 15: Simulation result for the HC BAR Chip with serpentine channel fins showing Temperature distribution in heating and cooling zone.

Figure 15 shows the capability of HC-BAR chip with the serpentine channel to avoid the effect of heating and cooling zone on each other. It can be observed that at the centre of the chip there is moderate temperature which is approx. 30°C. There is minimal effect of zones on each other.

X. DISCUSSION

In order to maintain the temperature of the target volume we need to calculate the heat required to travel from the helical channel to the target volume in case of the heating zone and from the target volume to helical channels in case of the cooling zone. This extracted heat can be given by 'Q' which can be calculated as

$$\mathbf{Q = m\ C\ \Delta T}$$

where '**C**' for the fluid in the helix which is water in this study 4.184 J/g°C)
ΔT = required temperature – Actual temperature of the fluid.
'**m**' = mass of fluid in the target volume,
m = (Water density) x (volume of the channel confined inside the helical channel)
and,

To calculate the required fluid temperature in helical channels we can apply Fourier's law of conduction

$$\mathbf{Q = -k\ A\ (T_H - T_T)/t}$$

where **A** = Area of the target volume confined inside the helical channels,
$\mathbf{T_T}$ = Fluid temperature in at Target volume,
$\mathbf{T_H}$ = Required Temperature of fluid in Helical channel,
t = distance between target volume and helical channel (average radius of the helix)

The overall efficiency of the HC BAR chip is satisfactory as it was able to elevate the temperature of the target volume by 22°C and lower it back by 20°C. It was also able to keep the two zones unaffected by each other. The serpentine path also provides the target volume to properly mix and distribute the temperature of the temperature uniformly for the laminar flow mixing can only be done by breaking or changing the direction of the flow and by diffusion process in the flow. Therefore, the serpentine path increases the overall length of the channels which provides enough processing time for diffusion and heat transfer in a small space of chip. These equations were used to calculate an approx. temperature to start with.

XI. FUTURE WORK

The validation of the simulation result is necessary for the check of the effectivity and working of the HC BAR chip. In order to do that 3D printing of the chip is proposed with a Stereolithography (SLA) 3D printer with the polymer resin with similar thermal conductivity. SLA is proposed as the design of the Chip is complex and contains several channels (Anycubic's Photon S or similar) printer are proposed. A Digital light processing (DLP) 3D printer can also be used.

Table 2:Specification for the 3D printer

Specification for the 3D printer	
Printer Tech	LCD-based SLA 3D Printer
Printer Bed	115 x 65mm
Light source	UV
Layer Height	25 ~ 100um
Printing speed	20mm/h
Materials:	405um resin or similar

11.1 Proposed Testing for the Chip

The following testing is required for the chip effectively working after 3D printing:

- Dimensional inspection of the chip as per the 3D model. Connect the Tygon tube to the Tygon tube connectors to check if they are intact and well-printed.
- Proof test for any leakage and failure of the chip.
- Droplet generation by the droplet generation mechanism inside the chip

- Thermal distribution of the helical channel at the target volume with the help of an IR camera. Thermocouples are to be used to check the effect of the heating and cooling zones on each other. This can also be done by the IR camera.

XII. BIBLIOGRAPHY

[1] A. Shahidian, M. Ghassemi, J. Mohammadi, and M. Hashemi, “9 - Application of microfluidics in cancer treatment,” *ScienceDirect*, Jan. 01, 2020. https://www.sciencedirect.com/science/article/abs/pii/B9780128178096000091 (accessed Jan. 08, 2024).

[2] G. M. Whitesides, “The origins and the future of microfluidics,” *Nature*, vol. 442, no. 7101, pp. 368–373, Jul. 2006, doi: https://doi.org/10.1038/nature05058.

[3] M. D. Tarn and N. Pamme, “Microfluidics,” *ScienceDirect*, Jan. 01, 2014. https://www.sciencedirect.com/science/article/pii/B9780124095472053518?via%3Dihub (accessed Jan. 08, 2024).

[4] P. Watts and C. Wiles, “Micro reactors, flow reactors and continuous flow synthesis,” *Journal of Chemical Research*, vol. 36, no. 4, pp. 181–193, Apr. 2012, doi: https://doi.org/10.3184/174751912x13311365798808.

[5] C. M. Leung *et al.*, “A guide to the organ-on-a-chip,” *Nature Reviews Methods Primers*, vol. 2, no. 1, pp. 1–29, May 2022, doi: https://doi.org/10.1038/s43586-022-00118-6.

[6] B. Yılmaz and F. Yılmaz, “Lab-on-a-Chip Technology and Its Applications,” *Omics Technologies and Bio-Engineering*, pp. 145–153, 2018, doi: https://doi.org/10.1016/b978-0-12-804659-3.00008-7.

[7] M. J. Madou, *Fundamentals of Microfabrication and Nanotechnology, Three-Volume Set*. CRC Press, 2018. Accessed: Jan. 08, 2024. [Online]. Available: https://books.google.ca/books?hl=en&lr=&id=gPm7DwAAQBAJ&oi=fnd&pg=PP1&ots=dbkrP96V46&sig=JT5L0FS0SLSe_WfvAuNcsL2lGhk&redir_esc=y#v=onepage&q&f=false

[8] C. Iliescu, H. Taylor, M. Avram, J. Miao, and S. Franssila, “A practical guide for the fabrication of microfluidic devices using glass and silicon,” *Biomicrofluidics*, vol. 6, no. 1, p. 016505, Mar. 2012, doi: https://doi.org/10.1063/1.3689939.

[9] H. Becker and C. Gärtner, “Polymer microfabrication technologies for microfluidic systems,” *Analytical and Bioanalytical Chemistry*, vol. 390, no. 1, pp. 89–111, Nov. 2007, doi: https://doi.org/10.1007/s00216-007-1692-2.

[10] X. Li, D. R. Ballerini, and W. Shen, “A perspective on paper-based microfluidics: Current status and future trends,” *Biomicrofluidics*, vol. 6, no. 1, pp. 11301–1130113, Mar. 2012, doi: https://doi.org/10.1063/1.3687398.

[11] M. Torabinia, P. Asgari, U. S. Dakarapu, J. Jeon, and H. Moon, “On-chip organic synthesis enabled using an engine-and-cargo system in an electrowetting-on-dielectric digital microfluidic device,” *Lab on a Chip*, vol. 19, no. 18, pp. 3054–3064, Sep. 2019, doi: https://doi.org/10.1039/C9LC00428A.

[12] A. M. Elizarov, “Microreactors for radiopharmaceutical synthesis,” *Lab on a Chip*, vol. 9, no. 10, p. 1326, 2009, doi: https://doi.org/10.1039/b820299k.

[13] J. C. Jokerst, J. Emory, and C. S. Henry, “Advances in microfluidics for environmental analysis,” *Analyst*, vol. 137, no. 1, pp. 24–34, Jan. 2012, doi: https://doi.org/10.1039/c1an15368d.

[14] Y. T. Atalay *et al.*, “Microfluidic analytical systems for food analysis,” *Trends in Food Science & Technology*, vol. 22, no. 7, pp. 386–404, Jul. 2011, doi: https://doi.org/10.1016/j.tifs.2011.05.001.

[15] K. M. Horsman, J. M. Bienvenue, K. R. Blasier, and J. P. Landers, “Forensic DNA Analysis on Microfluidic Devices: A Review,” *Journal of Forensic Sciences*, vol. 52, no. 4, pp. 784–799, Jul. 2007, doi: https://doi.org/10.1111/j.1556-4029.2007.00468.x.

[16] H. Jiang, X. Weng, and D. Li, “Microfluidic whole-blood immunoassays,” *Microfluidics and Nanofluidics*, vol. 10, no. 5, pp. 941–964, Oct. 2010, doi: https://doi.org/10.1007/s10404-010-0718-9.

[17] Y. Zhang and P. Ozdemir, “Microfluidic DNA amplification—A review,” *Analytica Chimica Acta*, vol. 638, no. 2, pp. 115–125, Apr. 2009, doi: https://doi.org/10.1016/j.aca.2009.02.038.

[18] V. Jain, R. K. Dwivedi, and K. Muralidhar, “Closed EWOD-based low-cost portable thermal detection system for point-of-care applications,” *Sensors and Actuators A: Physical*, vol. 346, p. 113831, Oct. 2022, doi: https://doi.org/10.1016/j.sna.2022.113831.

[19] A. Lenshof and T. Laurell, “Continuous separation of cells and particles in microfluidic systems,” *Chemical Society Reviews*, vol. 39, no. 3, p. 1203, 2010, doi: https://doi.org/10.1039/b915999c.

[20] S. Mashaghi, A. Abbaspourrad, D. A. Weitz, and A. M. van Oijen, “Droplet microfluidics: A tool for biology, chemistry and nanotechnology,” *TrAC Trends in Analytical Chemistry*, vol. 82, pp. 118–125, Sep. 2016, doi: https://doi.org/10.1016/j.trac.2016.05.019.

[21] P. S. Dittrich and A. Manz, “Lab-on-a-chip: microfluidics in drug discovery,” *Nature Reviews Drug Discovery*, vol. 5, no. 3, pp. 210–218, Mar. 2006, doi: https://doi.org/10.1038/nrd1985.

[22] J. Nie *et al.*, “Vessel-on-a-chip with Hydrogel-based Microfluidics,” *Small*, vol. 14, no. 45, pp. 1802368–1802368, Oct. 2018, doi: https://doi.org/10.1002/smll.201802368.

[23] V. van Duinen, S. J. Trietsch, J. Joore, P. Vulto, and T. Hankemeier, “Microfluidic 3D cell culture: from tools to tissue models,” *Current Opinion in Biotechnology*, vol. 35, pp. 118–126, Dec. 2015, doi: https://doi.org/10.1016/j.copbio.2015.05.002.

[24] H. Yin and D. Marshall, “Microfluidics for single cell analysis,” *Current Opinion in Biotechnology*, vol. 23, no. 1, pp. 110–119, Feb. 2012, doi: https://doi.org/10.1016/j.copbio.2011.11.002.

[25] D. Gao, H. Liu, Y. Jiang, and J.-M. Lin, “Recent advances in microfluidics combined with mass spectrometry: technologies and applications,” *Lab on a Chip*, vol. 13, no. 17, p. 3309, 2013, doi: https://doi.org/10.1039/c3lc50449b.

[26] C. Rohde, F. Zeng, R. Gonzalez-Rubio, M. Angel, and Mehmet Fatih Yanik, “Microfluidic system for on-chip high-throughput whole-animal sorting and screening at subcellular resolution,” *Proceedings of the National Academy of Sciences of the United States of America*, vol. 104, no. 35, pp. 13891–13895, Aug. 2007, doi: https://doi.org/10.1073/pnas.0706513104.

[27] R. Seemann, M. Brinkmann, T. Pfohl, and S. Herminghaus, “Droplet-based microfluidics,” *Reports on Progress in Physics*, vol. 75, no. 1, p. 016601, Dec. 2011, doi: https://doi.org/10.1088/0034-4885/75/1/016601.

[28] S.-Y. Teh, R. Lin, L.-H. Hung, and A. P. Lee, “Droplet microfluidics,” *Lab on a Chip*, vol. 8, no. 2, p. 198, 2008, doi: https://doi.org/10.1039/b715524g.

[29] B. Zhao, X. Cui, W. Ren, F. Xu, M. Liu, and Z.-G. Ye, “A Controllable and Integrated Pump-enabled Microfluidic Chip and Its Application in Droplets Generating,” *Scientific Reports*, vol. 7, no. 1, p. 11319, Sep. 2017, doi: https://doi.org/10.1038/s41598-017-10785-1.

[30] L. Mazutis, J. Gilbert, W. L. Ung, D. A. Weitz, A. D. Griffiths, and J. A. Heyman, “Single-cell analysis and sorting using droplet-based microfluidics,” *Nature Protocols*, vol. 8, no. 5, pp. 870–891, Apr. 2013, doi: https://doi.org/10.1038/nprot.2013.046.

[31] A. S. Opalski, T. S. Kaminski, and P. Garstecki, “Droplet Microfluidics as a Tool for the Generation of Granular Matters and Functional Emulsions,” *KONA Powder and Particle Journal*, vol. 36, no. 0, pp. 50–71, Jan. 2019, doi: https://doi.org/10.14356/kona.2019004.

[32] D.-K. Kang, M. Monsur Ali, K. Zhang, E. J. Pone, and W. Zhao, “Droplet microfluidics for single-molecule and single-cell analysis in cancer research, diagnosis and therapy,” *TrAC Trends in Analytical Chemistry*, vol. 58, pp. 145–153, Jun. 2014, doi: https://doi.org/10.1016/j.trac.2014.03.006.

[33] H. T. Nguyen, M. Marquis, M. Anton, and S. Marze, “Studying the real-time interplay between triglyceride digestion and lipophilic micronutrient bioaccessibility using droplet microfluidics. 2 application to various oils and (pro)vitamins,” *Food Chemistry*, vol. 275, pp. 661–667, Mar. 2019, doi: https://doi.org/10.1016/j.foodchem.2018.09.126.

[34] D. Liu, H. Zhang, F. Fontana, J. T. Hirvonen, and H. A. Santos, “Microfluidic-assisted fabrication of carriers for controlled drug delivery,” *Lab on a Chip*, vol. 17, no. 11, pp. 1856–1883, 2017, doi: https://doi.org/10.1039/c7lc00242d.

[35] P. Pattanayak *et al.*, “Microfluidic chips: recent advances, critical strategies in design, applications and future perspectives,” *Microfluidics and Nanofluidics*, vol. 25, no. 12, Oct. 2021, doi: https://doi.org/10.1007/s10404-021-02502-2.

[36] S. Maher *et al.*, “Multifunctional microspherical magnetic and pH responsive carriers for combination anticancer therapy engineered by droplet-based microfluidics,” *Journal of Materials Chemistry B*, vol. 5, no. 22, pp. 4097–4109, Jun. 2017, doi: https://doi.org/10.1039/C7TB00588A.

[37] Z. Z. Chong, S. H. Tan, A. M. Gañán-Calvo, S. B. Tor, N. H. Loh, and N.-T. Nguyen, “Active droplet generation in microfluidics,” *Lab on a Chip*, vol. 16, no. 1, pp. 35–58, 2016, doi: https://doi.org/10.1039/c5lc01012h.

[38] P. Garstecki, M. J. Fuerstman, H. A. Stone, and G. M. Whitesides, “Formation of droplets and bubbles in a microfluidic T-junction—scaling and mechanism of break-up,” *Lab on a Chip*, vol. 6, no. 3, p. 437, 2006, doi: https://doi.org/10.1039/b510841a.

[39] T. Fu, Y. Wu, Y. Ma, and H. Z. Li, “Droplet formation and breakup dynamics in microfluidic flow-focusing devices: From dripping to jetting,” vol. 84, pp. 207–217, Dec. 2012, doi: https://doi.org/10.1016/j.ces.2012.08.039.

[40] P. Zhu, X. Tang, and L. Wang, “Droplet generation in co-flow microfluidic channels with vibration,” *Microfluidics and Nanofluidics*, vol. 20, no. 3, Feb. 2016, doi: https://doi.org/10.1007/s10404-016-1717-2.

[41] D. Hess, T. Yang, and S. Stavrakis, “Droplet-based optofluidic systems for measuring enzyme kinetics,” *Analytical and Bioanalytical Chemistry*, Dec. 2019, doi: https://doi.org/10.1007/s00216-019-02294-z.

[42] Chan Hee Chon and D. Li, “Temperature Control in Microfluidic Systems,” *Springer eBooks*, pp. 1976–1980, Aug. 2008, doi: https://doi.org/10.1007/978-0-387-48998-8_1530.

[43] A. A. Dos-Reis-Delgado *et al.*, “Recent advances and challenges in temperature monitoring and control in microfluidic devices,” *ELECTROPHORESIS*, vol. 44, no. 1–2, pp. 268–297, Oct. 2022, doi: https://doi.org/10.1002/elps.202200162.

[44] S. Srikanth, S. Raut, S. K. Dubey, I. Ishii, A. Javed, and S. Goel, “Experimental studies on droplet characteristics in a microfluidic flow-focusing droplet generator: effect of continuous phase on droplet encapsulation,” *The European Physical Journal E*, vol. 44, no. 8, Aug. 2021, doi: https://doi.org/10.1140/epje/s10189-021-00115-9.

[45] T. N. D. Trinh, H. D. K. Do, N. N. Nam, T. T. Dan, K. T. L. Trinh, and N. Y. Lee, “Droplet-Based Microfluidics: Applications in Pharmaceuticals,” *Pharmaceuticals*, vol. 16, no. 7, p. 937, Jul. 2023, doi: https://doi.org/10.3390/ph16070937.

[46] C. Fang, D. Lee, B. Stober, G. G. Fuller, and A. Q. Shen, “Integrated microfluidic platform for instantaneous flow and localized temperature control,” *RSC Advances*, vol. 5, no. 104, pp. 85620–85629, Oct. 2015, doi: https://doi.org/10.1039/C5RA19944A.

[47] D. Sanchez, G. Nordin, and T. Munro, “Microfluidic Temperature Behavior in a Multi-Material 3D Printed Chip,” *Asme.org*, 2024. https://asmedigitalcollection.asme.org/IMECE/proceedings/IMECE2019/59476/V010T12A001/1073485 (accessed Jan. 08, 2024).

[48] T. Munro *et al.*, “3D printing-enabled uniform temperature distributions in microfluidic devices,” *Lab on a Chip*, vol. 22, no. 22, pp. 4393–4408, Nov. 2022, doi: https://doi.org/10.1039/D2LC00612J.

[49] “Model and Simulate Microfluidics Devices,” COMSOL. https://www.comsol.com/microfluidics-module (accessed Jan. 08, 2024).

[50] F. Kreith and R. M. Manglik, Principles of heat transfer. Boston, Ma Cengage Learning, 2018.